Transport and acceleration of plasma in the inner magnetosphere

Natalia Ganushkina (1, 2) and Michael Liemohn (2)

(1) Finnish Meteorological Institute, Helsinki, Finland/

(2) University of Michigan, Ann Arbor MI, USA

The research leading to these results was partly funded by the European Union Seventh Framework Programme (FP7/2007-2013) under grant agreement No 262468 SPACECAST andNo 606716 SPACESTORM

40th COSPAR Scientific Assembly 2014, Moscow, Russia, 2 - 10 August 2014

Transport and acceleration of plasma in the inner magnetosphere

Natalia Ganushkina (1, 2) and Michael Liemohn (2)

(1) Finnish Meteorological Institute, Helsinki, Finland/
(2) University of Michigan, Ann Arbor MI, USA

The part of the research leading to these results has received funding from the European Union Seventh Framework Programme (FP7/2007-2013) under grant agreement No 262468 **SPACECAST** and No 606716 **SPACESTORM**

40th COSPAR Scientific Assembly 2014, Moscow, Russia, 2 - 10 August 2014

Dynamical inner magnetosphere: Overview

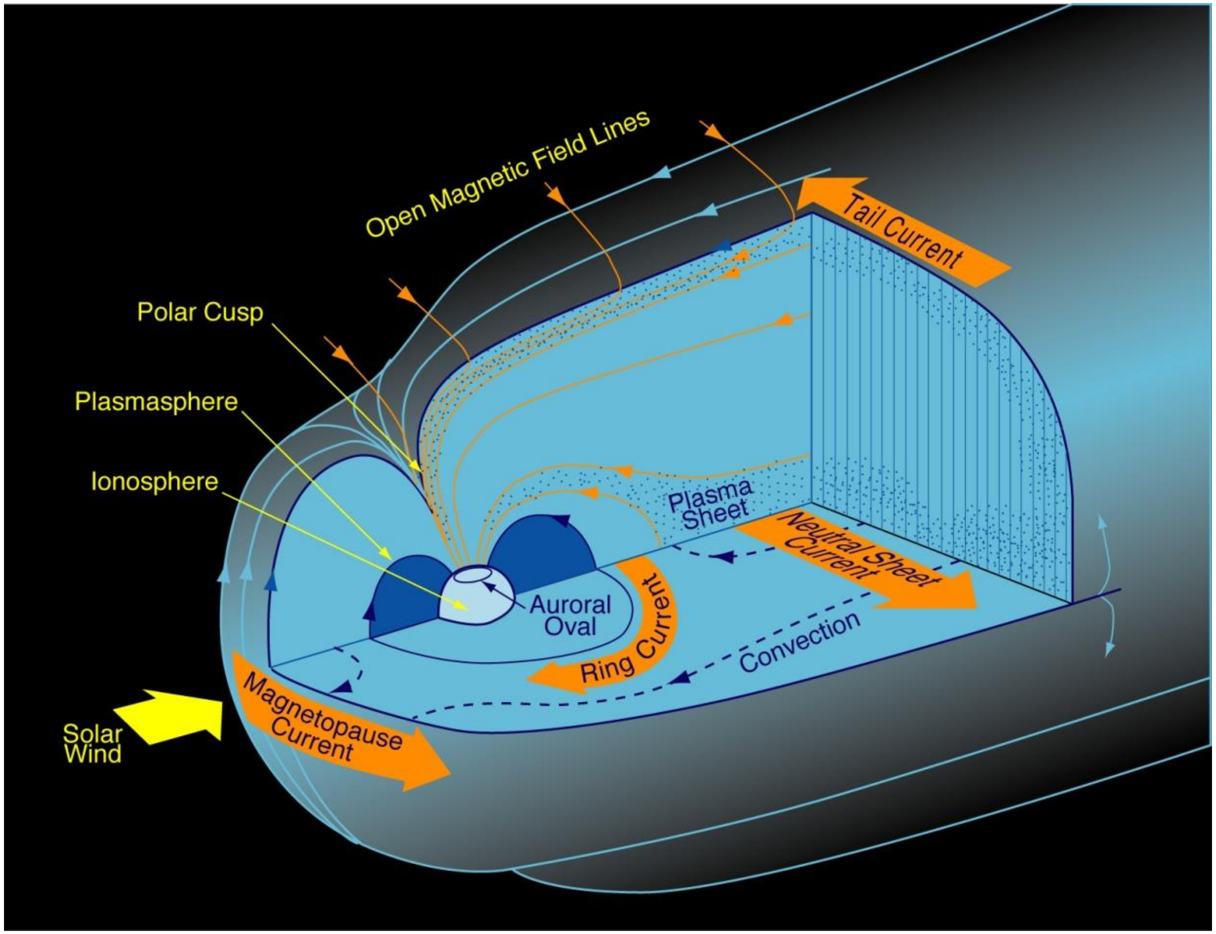

Plasma in magnetosphere:
mainly electrons and ions.

Sources of particles:
solar wind and ionosphere.

Plasma is grouped into different regions with different densities and temperatures.

Main regions:
- near Earth **plasma sheet** (7-10 Re, n = 0.1-1 cm^{-3}, T=5 keV)
- **field-aligned currents** (~ 10^6 A)
- **plasmasphere** (< 4 Re, 10^3 cm^{-3}, 1 eV)
- **plasmapause** (sharp at 4 Re, drop to 1 cm^{-3})
- **ring current** (20-300 keV)
- **radiation belts** (up to MeVs) (2-7 Re)

Sources of the inner magnetosphere particles

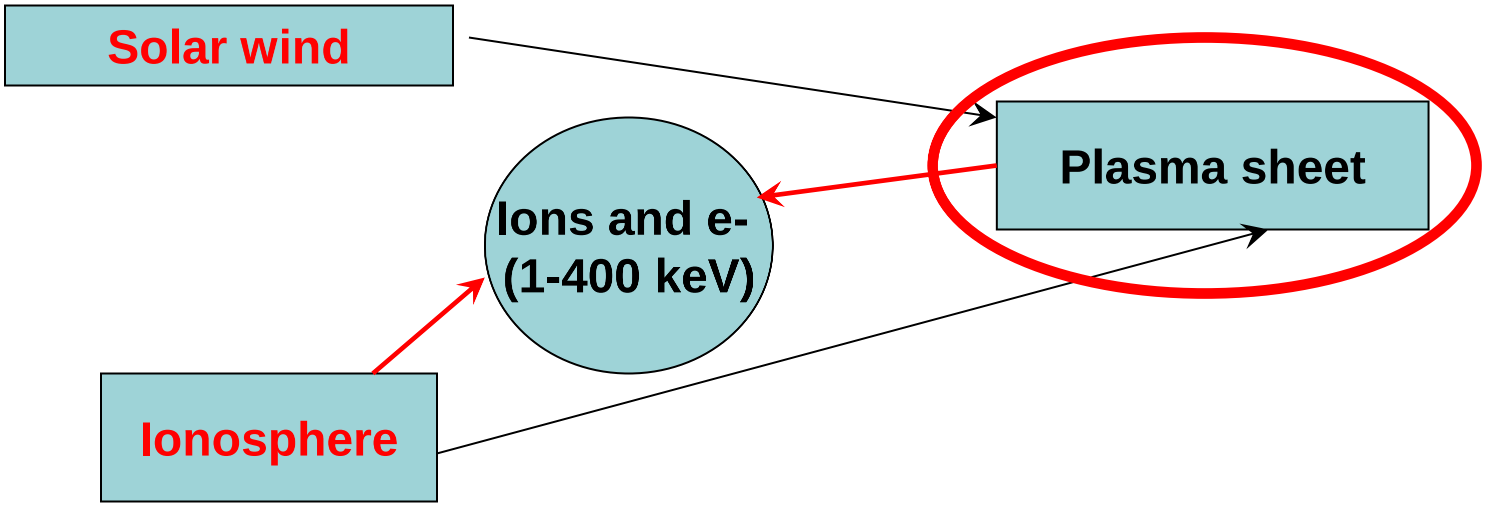

Origin of ion species:

- magnetospheric H+ ions: from ionosphere and solar wind (this complicates identification of the dominant source);
- majority of magnetospheric O+: ionosphere;
- He++: solar wind;
- He+: ionosphere.

Charge-exchange transforms solar wind higher charge state O ions to ionosphere-like lower charge state, solar wind He++ into He+ (provided by the ionosphere).

Large-scale convection:
Source of plasma and electric field in the magnetosphere

Existing models: *Volland-Stern, McIlwain, Weimer, RCM*

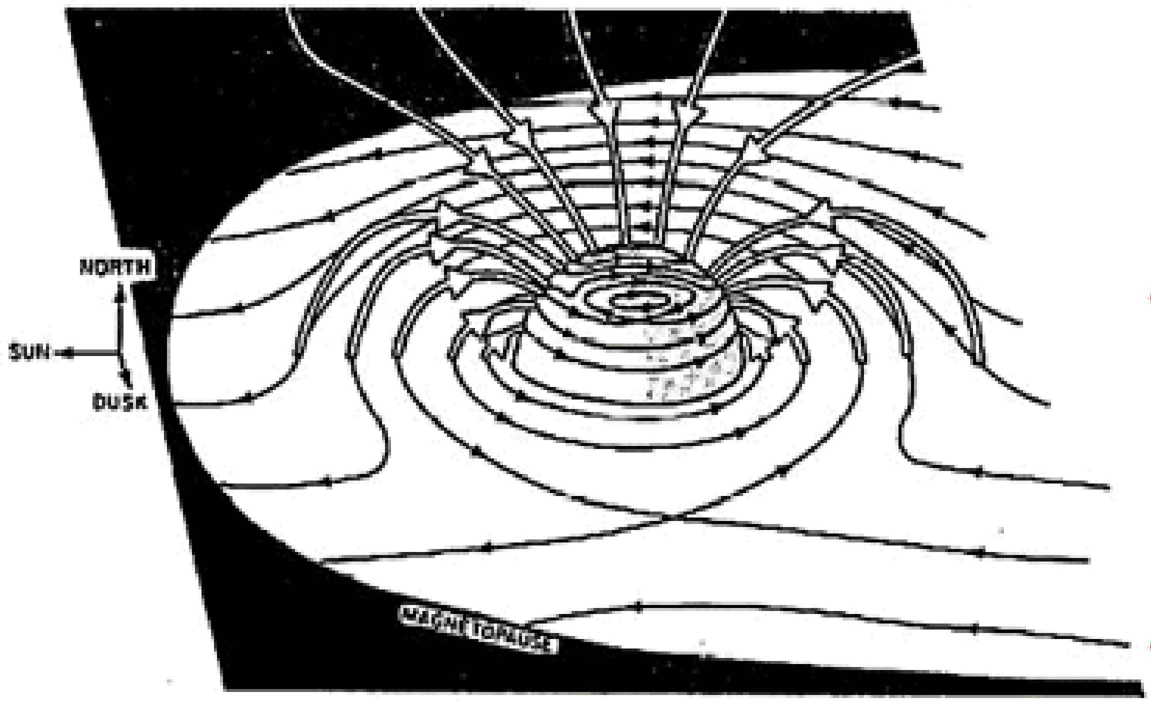

after Hill T. W. and R. A. Wolf, Solar-Wind Interactions in The Upper Atmosphere and Magnetosphere, National Academy of Sciences, Washington, D.C., pgs. 25-41, 1977

- **Typical convection pattern in the magnetosphere, mapped to the topside ionosphere in the northern hemisphere.**
- **The solid lines represent flow lines for the low temperature plasma projected on the equatorial plane & the earth's surface.**
- **Open lines are representative magnetic field lines in the noon-midnight plane**

Earthward transport of plasma in form of short-duration, high-speed plasma flows

Angelopoulos et al., JGR, 1992

Earthward transport of plasma and magnetic flux occurs in form of short-duration, high-speed plasma flows (*Baumjohann et al., 1990; Angelopoulos et al., 1992*).

“The high-speed flows organize themselves in 10-min time scale flow enhancements called bursty bulk flow (BBF) events.
The flow velocity exhibits peaks of very large amplitude with a characteristic time scale of the order of a minute, which are usually associated with magnetic field dipolarizations and ion temperature increases.

The BBFs represent intervals of enhanced earthward convection and energy transport. “

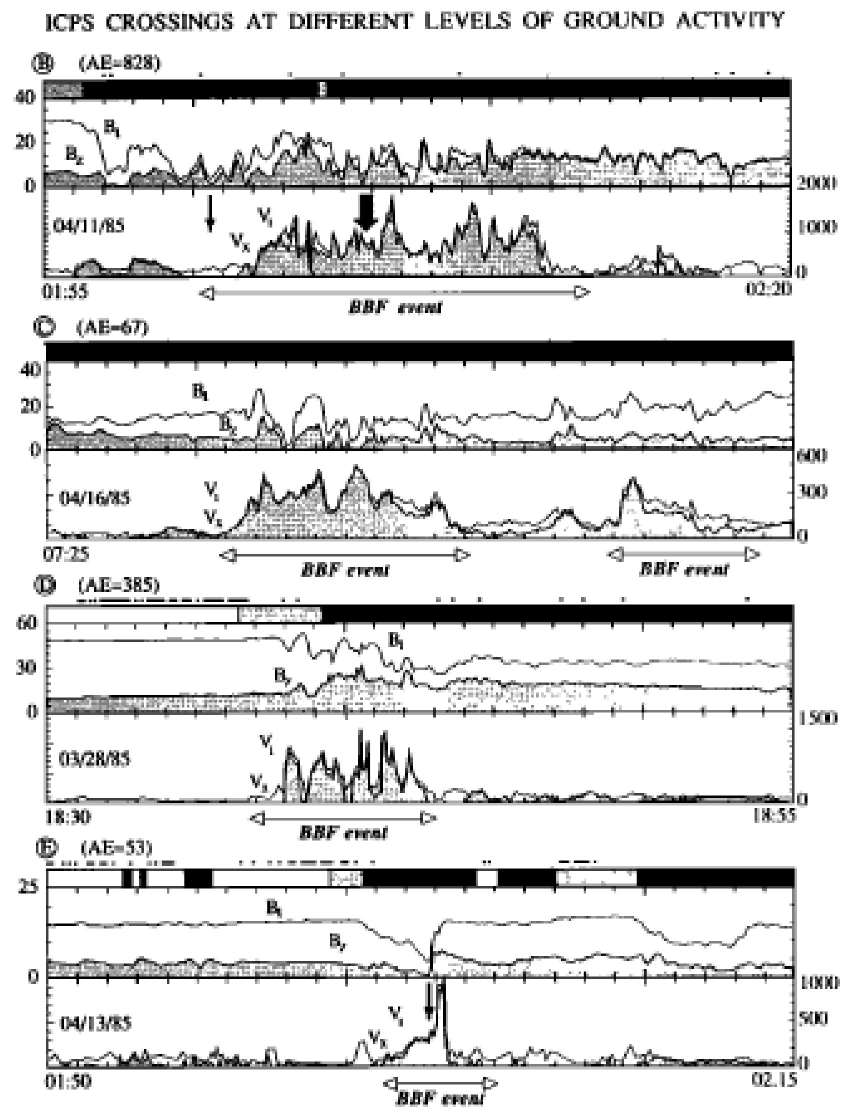

Substorms, injections and impulsive electric fields

Tu et al., JGR, 2000

Energetic particle **injections** are important manifestations of substorm expansion phase (*Arnoldy and Chan, 1969; Belian et al., 1978, 1984; Reeves et al., 1991*).

Electric field behavior is important for understanding of particle injections:
  - **Intense (a few mV/m) electric fields** with a strong pulsed component detected deep in the inner magnetosphere during substorms *(Sheperd et al., 1980; Aggson et al., 1983; Maynard et al., 1983, 1996; Tu et al., 2000*).

  - Simulations (*Birn et al., 1997; Li et al., 1998; Ganushkina et al., 2005, 2006, 2012*) suggested these fields important for transport and acceleration during substorms.

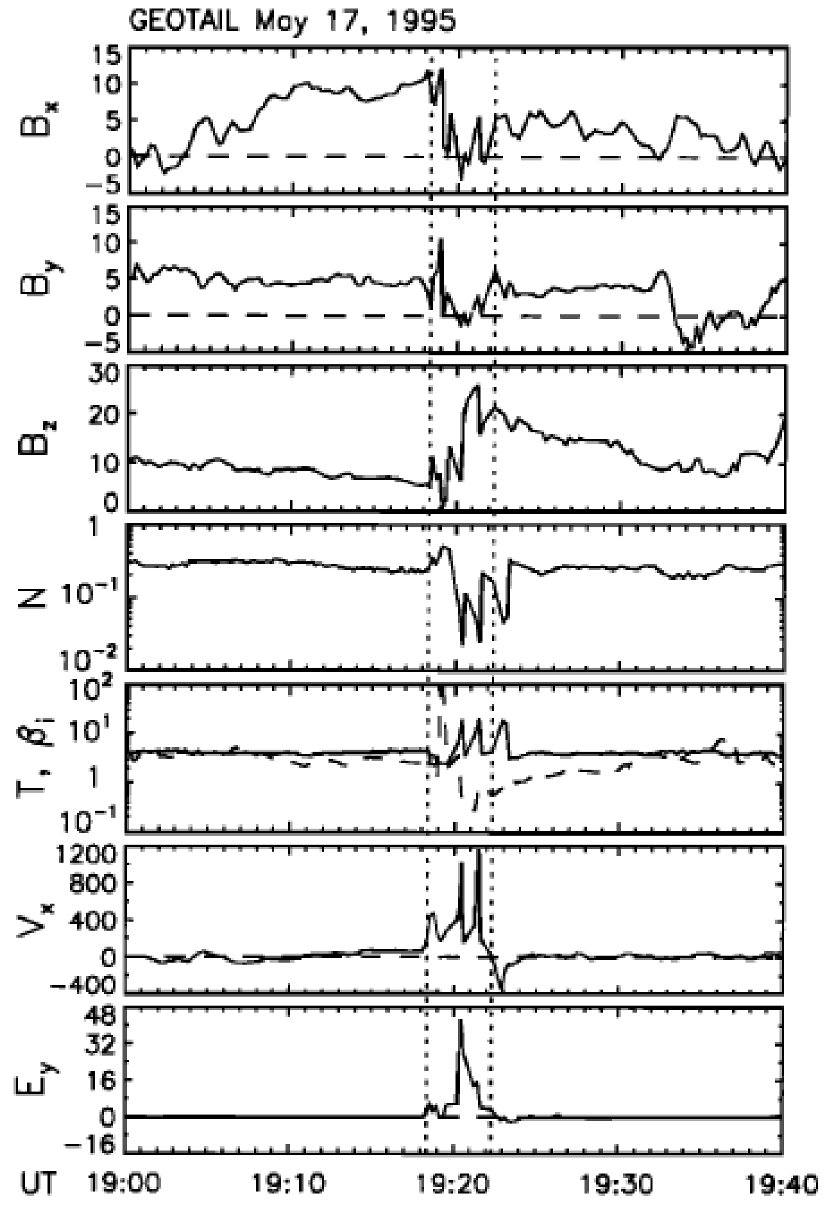

Intense nose structures: November 3, 1997 event

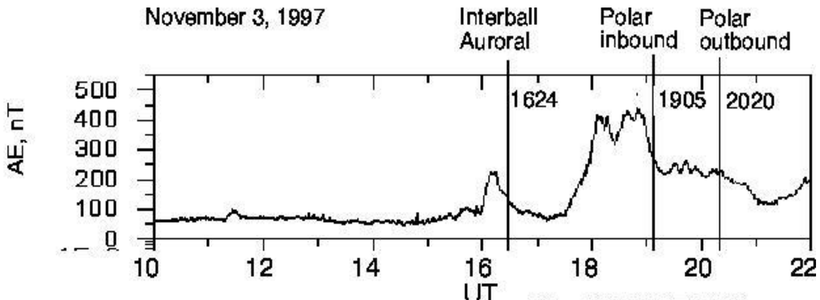

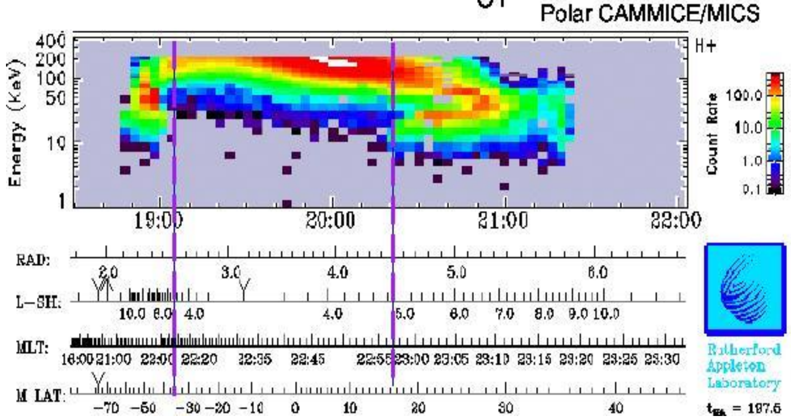

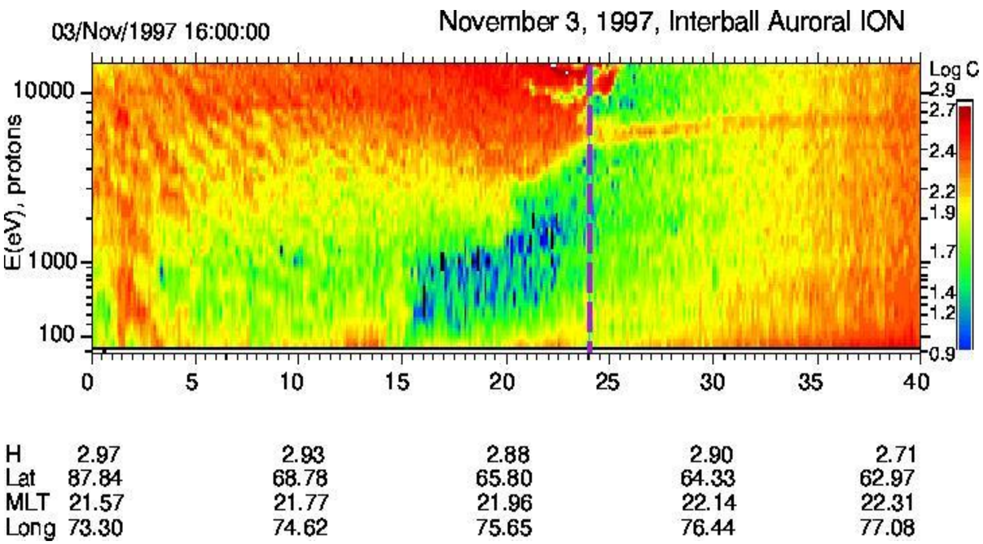

Satellite	UT	Req	MLT
Interball Auroral	1624	6.73	2200
LANL	1755	6.6	0100
Polar/ Inbound	1900	4.7	2158
Polar/ Outbound	2020	4.86	2254

Interball Auroral nose:
location of plasma for Polar/inbound nose formation 2.5 hours later.

LANL: indicator of inward plasma transport.

1755 UT, L=6.6 $\rightarrow$ 1900 UT, L=4.7 $\Rightarrow$
2 Re inward motion within 1 hour.

(Ganushkina et al., JGR, 2000)

Inner Magnetosphere Particle Transport and Acceleration Model (IMPTAM)

(*Ganushkina et al., 2001, 2005, 2006, 2012***)**

The inner magnetosphere particle transport and acceleration model:
- follows distributions of ions and electrons with arbitrary pitch angles
- from the plasma sheet to the inner L-shell regions
- with energies reaching up to hundreds of keVs
- in time-dependent magnetic and electric fields.
- distribution of particles is traced in the guiding center, or drift, approximation
  (motion of a charged particle as displacements of its guiding center,
  or the center of the circular Larmor orbit of a moving particle).

In order to follow the evolution of the particle **distribution function** f and particle **fluxes** in the inner magnetosphere dependent on the **position, time, energy, and pitch angl**e , it is necessary to specify:

(1) particle distribution at initial time at the model boundary;
(2) magnetic and electric fields everywhere dependent on time;
(3) drift velocities;
(3) all sources and losses of particles.

Inner Magnetosphere Particle Transport and Acceleration Model (2)

Changes in the distribution function f (R, φ, t, E, α), where R and φ are the radial and azimuthal coordinates in the equatorial plane, respectively, t is the time, E is the particle energy, α is the particle pitch angle, are obtained by:

$$\frac{df}{dt} = \frac{\partial f}{\partial \phi} \cdot V_\phi + \frac{\partial f}{\partial r} \cdot V_r + sources - losses$$

where V_φ and V_R are the azimuthal and radial components of the bounce-average drift velocity.

Transport of particles:

Drifts with velocities, radial and longitudinal, as sum of **ExB and magnetic drifts**

$$\mathrm{Vdrift} = \frac{\vec{E} \times \vec{B}}{B^2} + \frac{m v_\perp^2}{2 q B^3}\left(\vec{B} \times \nabla B\right) + \frac{m v_{II}^2}{q} \frac{\vec{R}_c \times \vec{B}}{R_c^2 B^2}$$

1st and 2nd adiabatic invariants conserved.

Inner Magnetosphere Particle Transport and Acceleration Model (3)

Boundary distribution: at any location from 6.6 to 10 Re
The particle distribution at the boundary is defined as a Maxwellian or kappa distribution function with parameters obtained from the empirical relations or from the observations during specific events.

Losses for ions:

- **charge exchange** with Hydrogen from geocorona;
- **Coulomb interaction** in dense thermal plasmas (plasmasphere);
- **convection outflow**, particle intersects the magnetopause and flows away along magnetosheath magnetic field lines.

Models to explain particle injections

♦ Injection front model (*Moore et al., 1981; Mauk and Meng*, 1983):
Particles are transported towards the Earth by **a compressional wave** front that propagates earthward from a disturbance occurring in the magnetotail. Propagation speed of 150 km/s between 9 and 6.6 Re (*Russell and McPherron, 1973*)

.

♦ Solving MHD equations (Birn *et al., 1997; 1998; Kim et al., 2000):* the results strongly depend on the assumed plasma sheet and substorm parameters in the MHD simulation

♦ Taking a difference between two different vector potentials of a model magnetic field gives induction electric field (*Quinn and Southwood,1982; Delcourt et al., 1990; Fok et al., 1996;1999; Bourdarie et al., 2000).*

♦ Assuming the electric field explicitly (Sergeev *et al*., *1998; Ebihara et al*.,1998; *Gabrielse et al*., 2012).

♦ Electromagnetic pulse model (*Li et al*., 1993, 1998*; Zaharia et al*., 2000, 2004*; Sarris et al*., 2002)
An **earthward propagating pulse** with constant velocity of westward E and corr. B
Good agreement with the observed dispersionless electron injections at geostationary orbit *(Ingraham et al*., 2001*; Li et a*l., 2003, *Mithaiwala et al*., 2005, *Liu et al*., 2009; *Ganushkina et a*l., 2013, 2014)

Electric field pulse model

Time varying fields associated with dipolarization in magnetotail, modeled as an electromagnetic pulse (*Li et al., 1998; Sarris et al., 2002*):

- Perturbed fields propagate from tail toward the Earth;
- Time-dependent Gaussian pulse with azimuthal E;
- E propagates radially inward at a decreasing velocity;
- decreases away from midnight.

Time-dependent B from the pulse is calculated by Faraday's law.

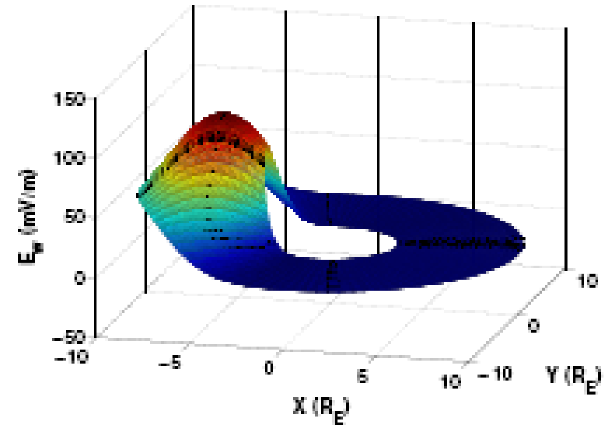

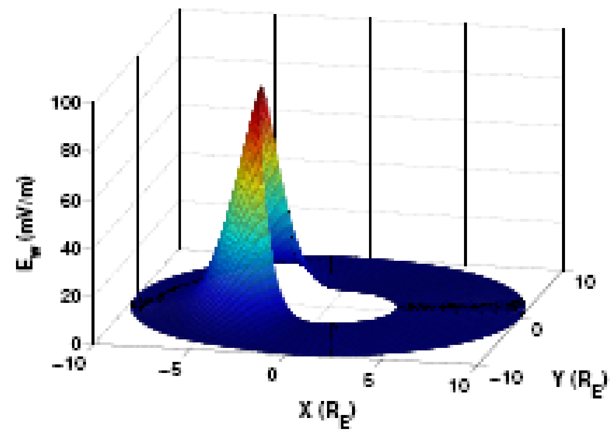

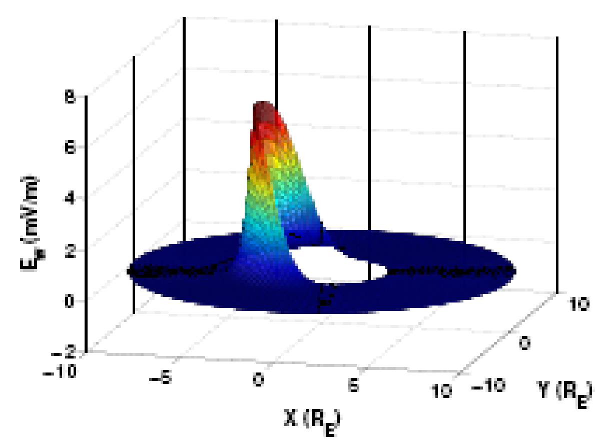

Intense nose structures: November 3, 1997 event

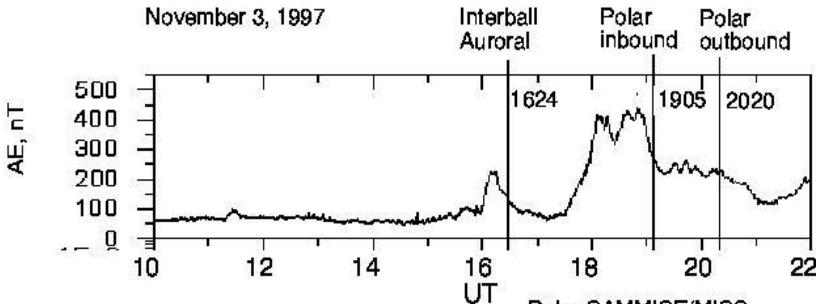

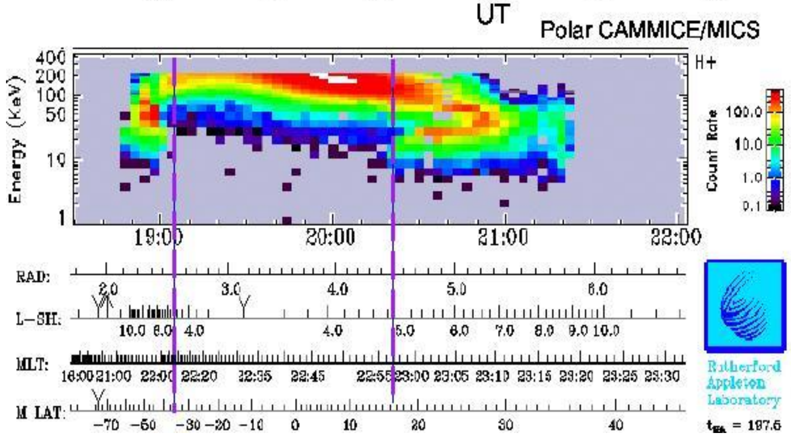

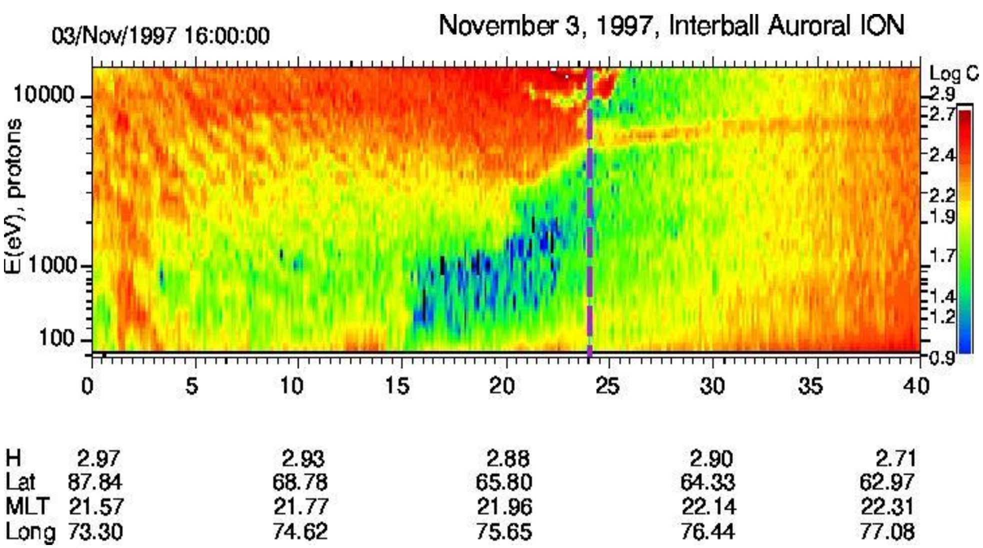

Satellite	UT	Req	MLT
Interball Auroral	1624	6.73	2200
LANL	1755	6.6	0100
Polar/ Inbound	1900	4.7	2158
Polar/ Outbound	2020	4.86	2254

Interball Auroral nose:
location of plasma for Polar/inbound nose formation 2.5 hours later.

LANL: indicator of inward plasma transport.

1755 UT, L=6.6 → 1900 UT, L=4.7 ⇒
2 Re inward motion within 1 hour.

(Ganushkina et al., JGR, 2000)

Regular and Intense nose structures

VS+T89, Kp=1

VS+T89+pulse (1mV/m), Kp=1

after 2 h

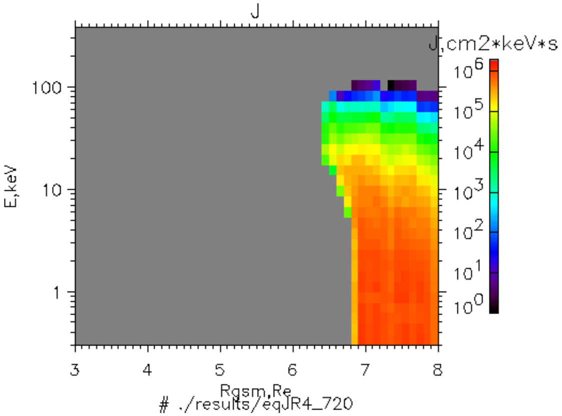

after 2 h

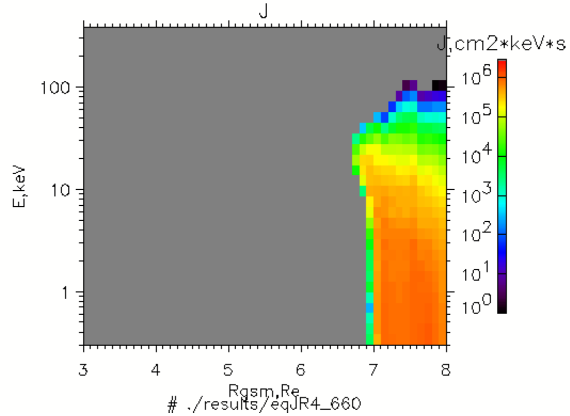

after 2 h 10 min

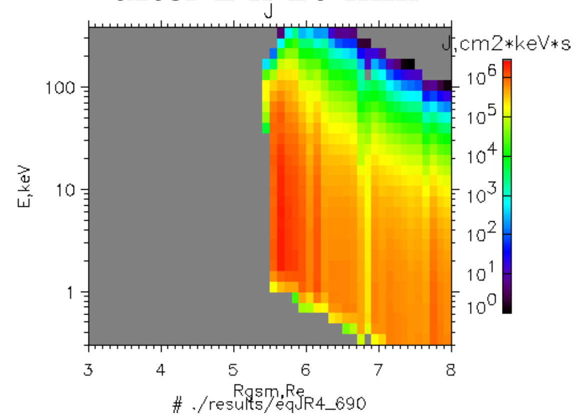

after 10 h

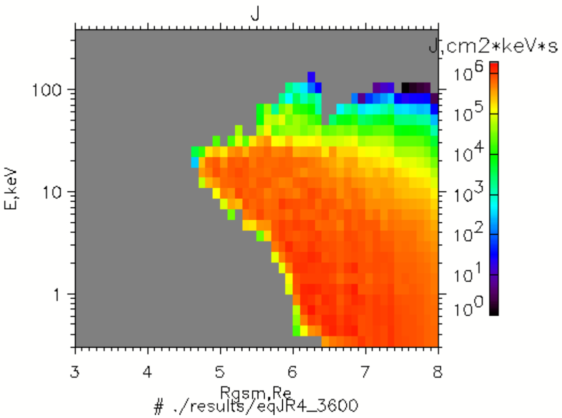

after 3 h 30 min

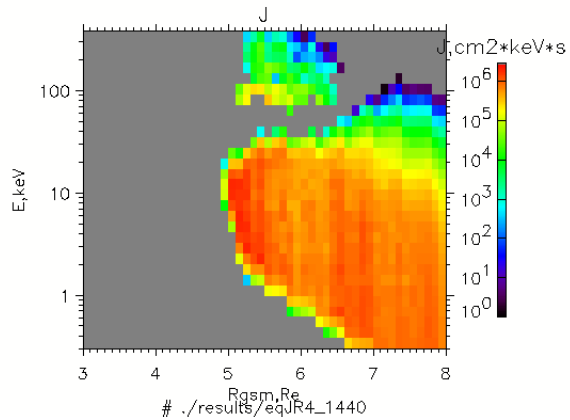

(Ganushkina et al., GRL, 2001)

large-scale convection and corotation, long formation times (10-20 hours).

fast earthward shift of previous population by **impulsive electric field** associated with substorm dipolarization, 2 Re for about 1 hour,

Ring current development

Relative importance of large-scale convection and substorm-associated electric fields for ring current development is still an issue under discussion

- Storms as superposition of substorms (*Chapman, 1962; Akasofu, 1966*);

- Substorm occurrence is incidental to storm main phase (*Kamide*, 1992);

- Convection paradigm: Particle transport and acceleration are due to a large-scale and long-standing convection electric field most likely driven by the solar wind (*Lee et al., 1983; Wodnicka, 1989; Takahashi et al., 1990; Kozyra et al., 1998; Ebihara and Ejiri, 1998, 2000; Jordanova et al., 2001; Liemohn et al., 1999, 2001*);

- Substorm paradigm: Particle transport and acceleration are due to a localized and short-lived impulsive electric field lasting several tens minutes (*Fok et al., 1996; Ebihara et al., 1998*).

- Concurrent action of convection and substorm-associated field variations (*Fok et al., 1999; Ganushkina et al., 2005; 2006*)

Contributions to RC energy from protons with different energy ranges: 27 storms' statistics from Polar CAMMICE/MICS data

(*Ganushkina et al., 2005*)

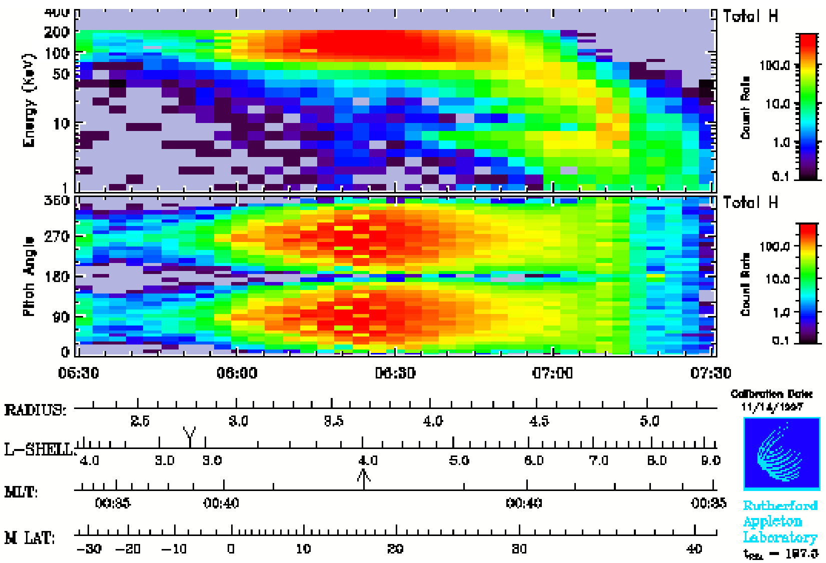

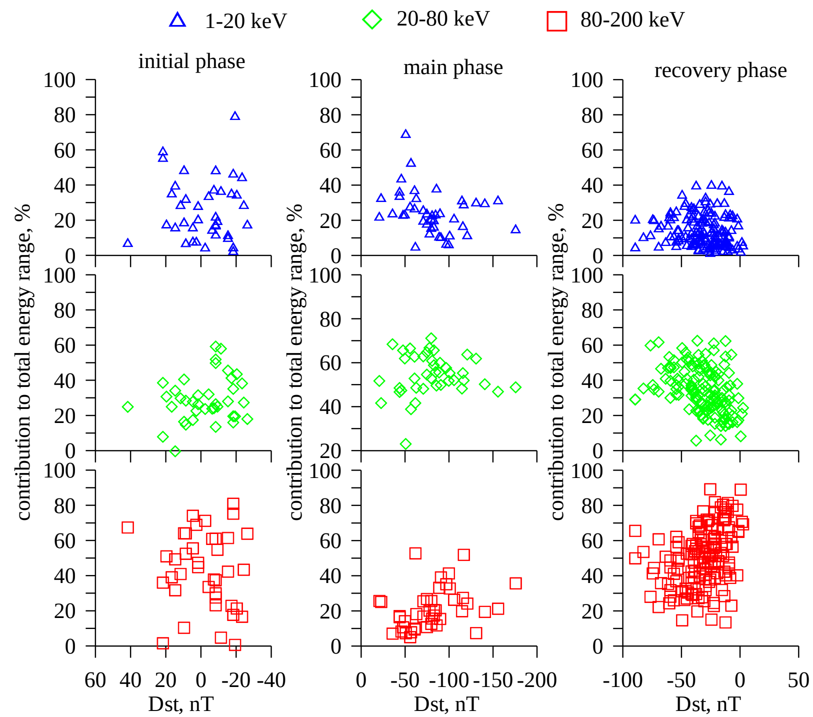

<u>Polar orbit, years 1996-1998</u>

- 1.8 x 9 Re, 86º incl.,
- 18 h period,
- ions of 1-200 keV

<u>Storm main phase</u>: **<u>medium</u>** energies (20-80 keV)

<u>Storm recovery phase</u>: **<u>high</u>** energies (80-200 keV)

October 21-23, 2001 storm: Energy density

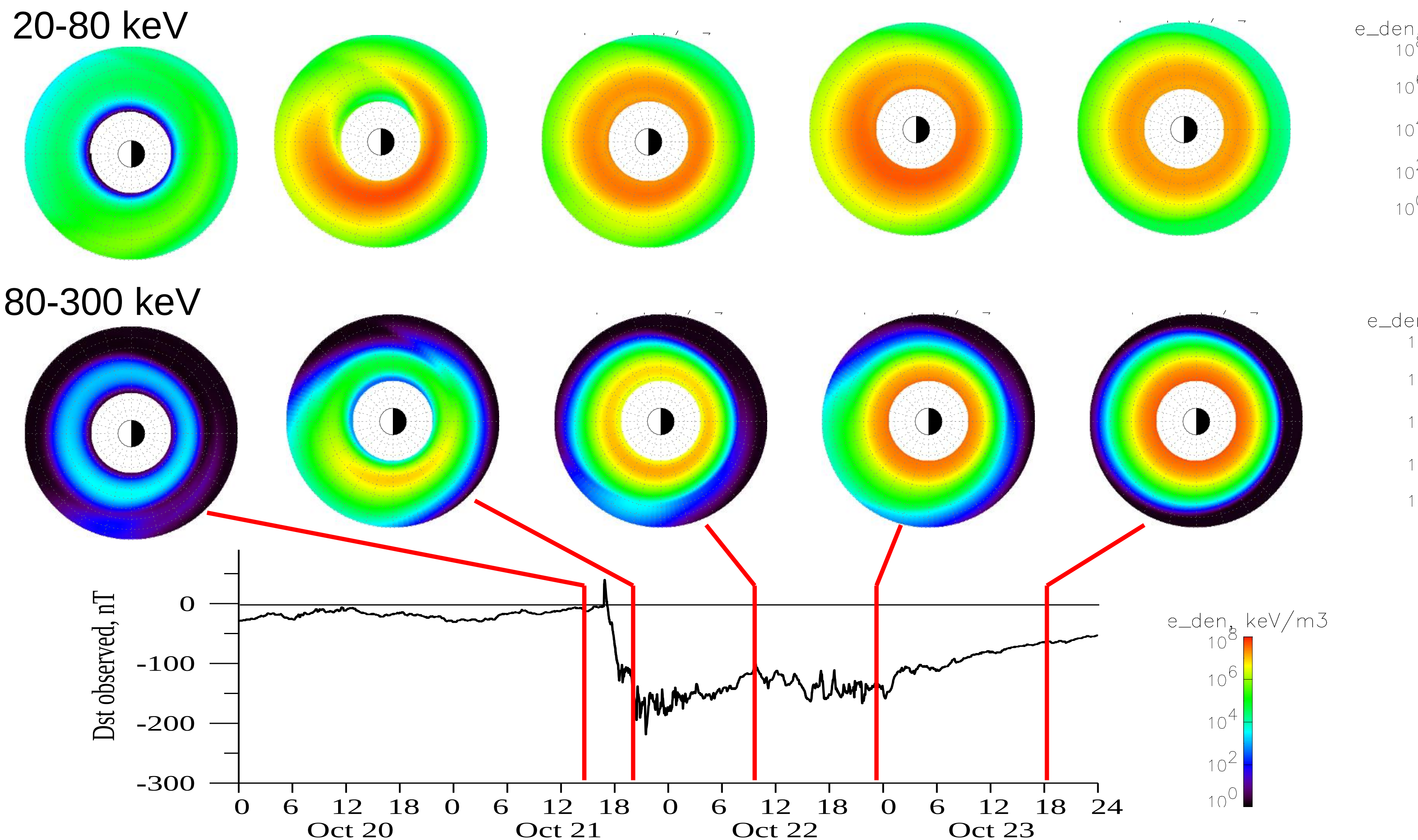

Ganushkina and Pulkkinen, ASR, 2002

October 21-23, 2001 storm: Pulsed e-m field

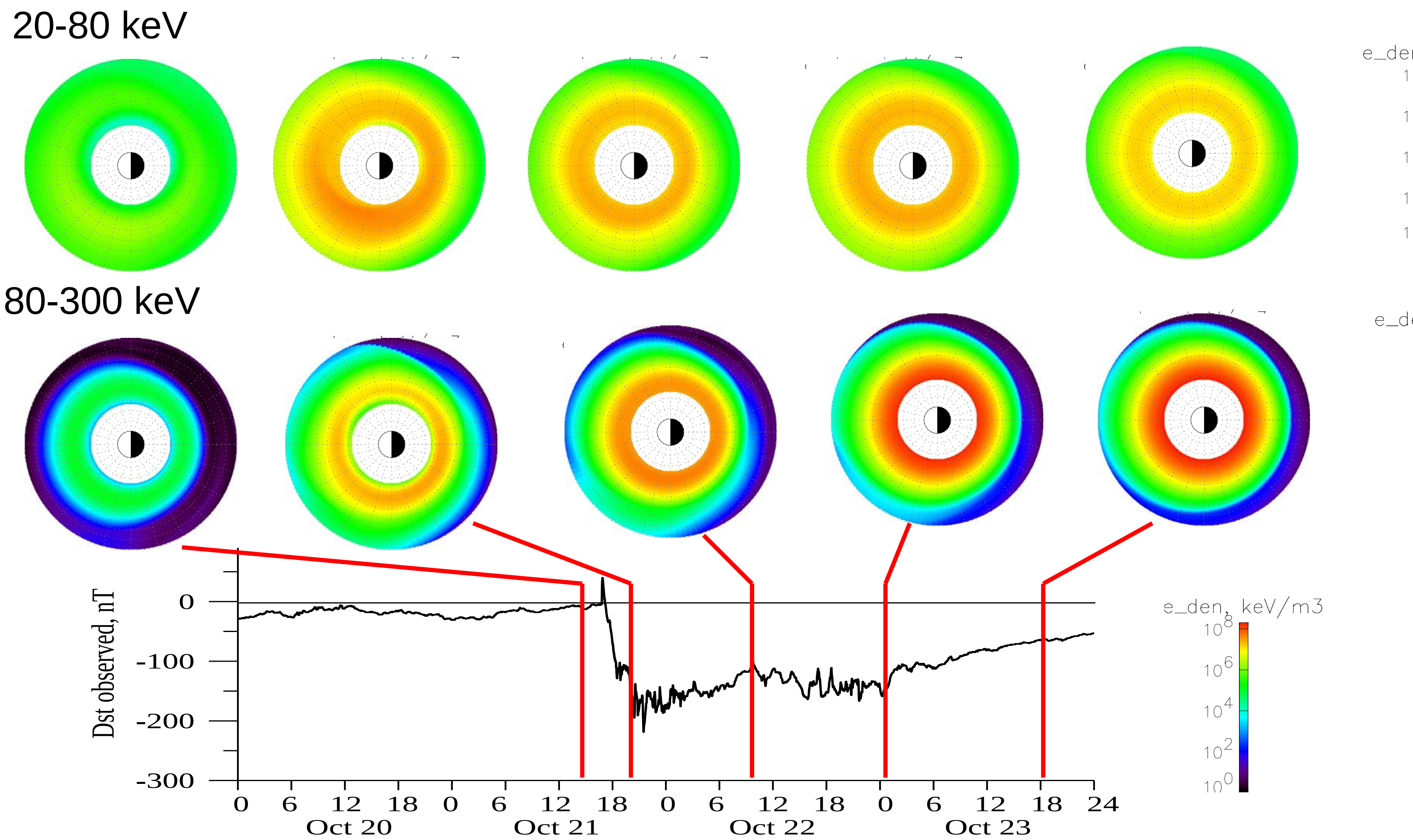

Ganushkina and Pulkkinen, ASR, 2002

Low energy electrons in the inner magnetosphere

- The distribution of low energy electrons, the seed population (10 to few hundreds of keV), is critically important for radiation belt dynamics.

- Surface charging by electrons with < 100 keV can cause significant damage and spacecraft anomalies (*Purvis et al*., 1984; *Whipple*, 1981; *Garrett* , 1981; *Davis et al*., 2008; *Frezet et al*., 1988; *Hoeber et al*., 1998; *Koons et al*., 1999).

- Simple corotation and convection electric field can describe rather well the average properties of transport for low energy electrons as Kp-dependent in the inner magnetosphere (*Korth et al*., 1999; *Friedel et al*., 2001; *Thomsen et al*., 2002; *Kurita et al*., 2011).

- Storm time dipolarization events result in strong radial transport and energization of radiation belt electrons (*Mauk and Meng*, 1983; *Kerns et al*., 1994; *Ingraham et al*., 2001; *Li et al*., 2003; *Mithaiwala and Horton*, 2005; *Miyoshi et al*., 2006; *Shprits et al*., 2009; *Liu et al*., 2009; *Glocer et al*., 2011).

Inner Magnetosphere Particle Transport and Acceleration Model for low energy electrons

Radial diffusion is applied (*Schulz and Lanzerotti*, 1974)

$$\frac{df}{dt} = L^2 \frac{\partial}{\partial L}\left(\frac{1}{L^2} D_{LL} \frac{\partial f}{\partial L}\right) - \frac{f}{\tau}$$

with diffusion coefficients D_{LL} (*Brautigam and Albert*, 2000): $D_{LL} = 10^{0.056Kp-9.325} L^{10}$

Losses for electrons:

- **convection outflow**, particle intersects the magnetopause and flows away along magnetosheath magnetic field lines;
- scattering into the loss cone due to **pitch angle diffusion** by introducing electron lifetimes:

. by *Chen et al*. (2005) for strong diffusion

$$\tau_{sd} = \left(\frac{\gamma m_0}{p}\right)\left[\frac{2\Psi B_h}{1-\eta}\right]$$

and *Shprits et al*. (2007) for weak diffusion

$$\tau_{wd} = 4.8 \cdot 10^4 B_w^{-2} L^{-1} E^2, \quad B_w^2 = 2 \cdot 10^{2.5+0.18Kp}$$

Electric field pulse model

Time varying fields associated with dipolarization in magnetotail, modeled as an electromagnetic pulse (*Li et al., 1998; Sarris et al., 2002*):

- Perturbed fields propagate from tail toward the Earth;
- Time-dependent Gaussian pulse with azimuthal E;
- E propagates radially inward at a decreasing velocity;
- decreases away from midnight.

Time-dependent B from the pulse is calculated by Faraday's law.

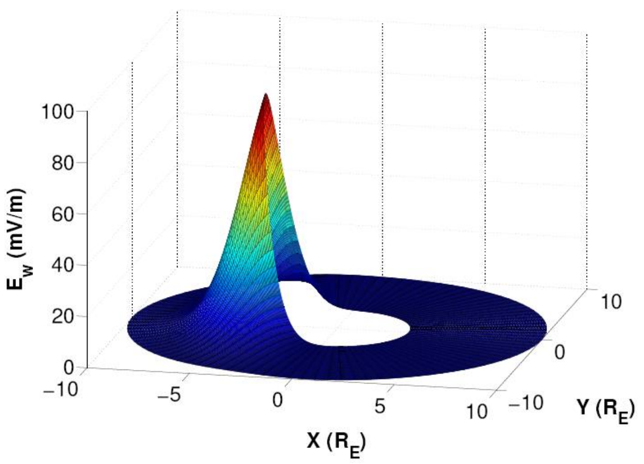

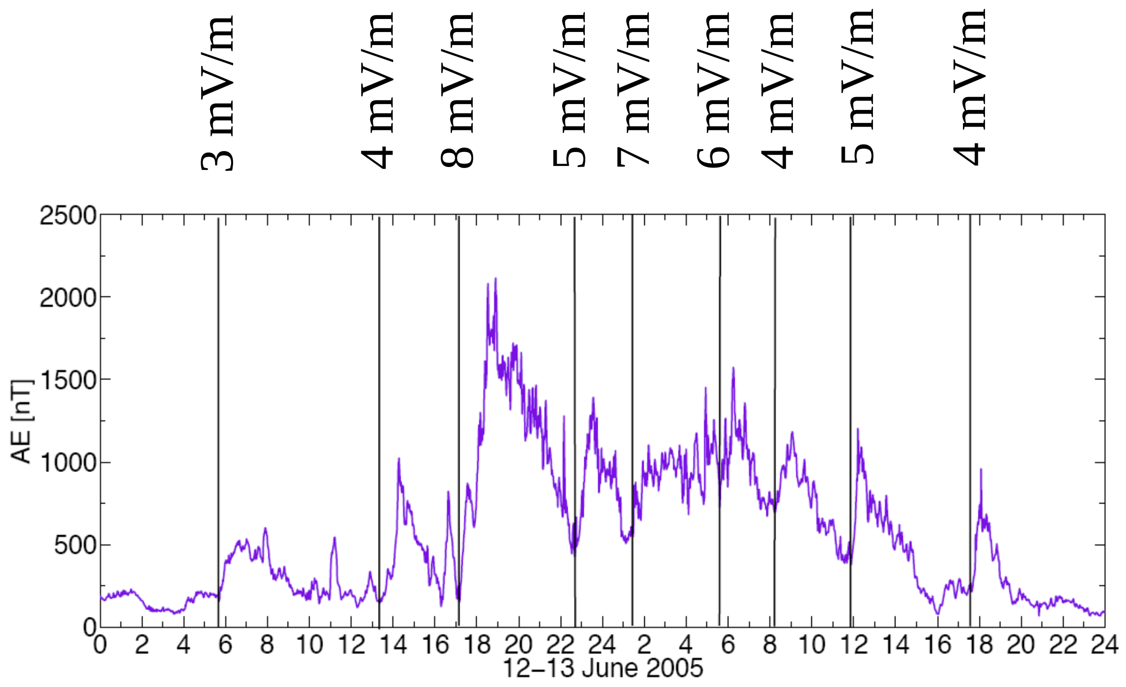

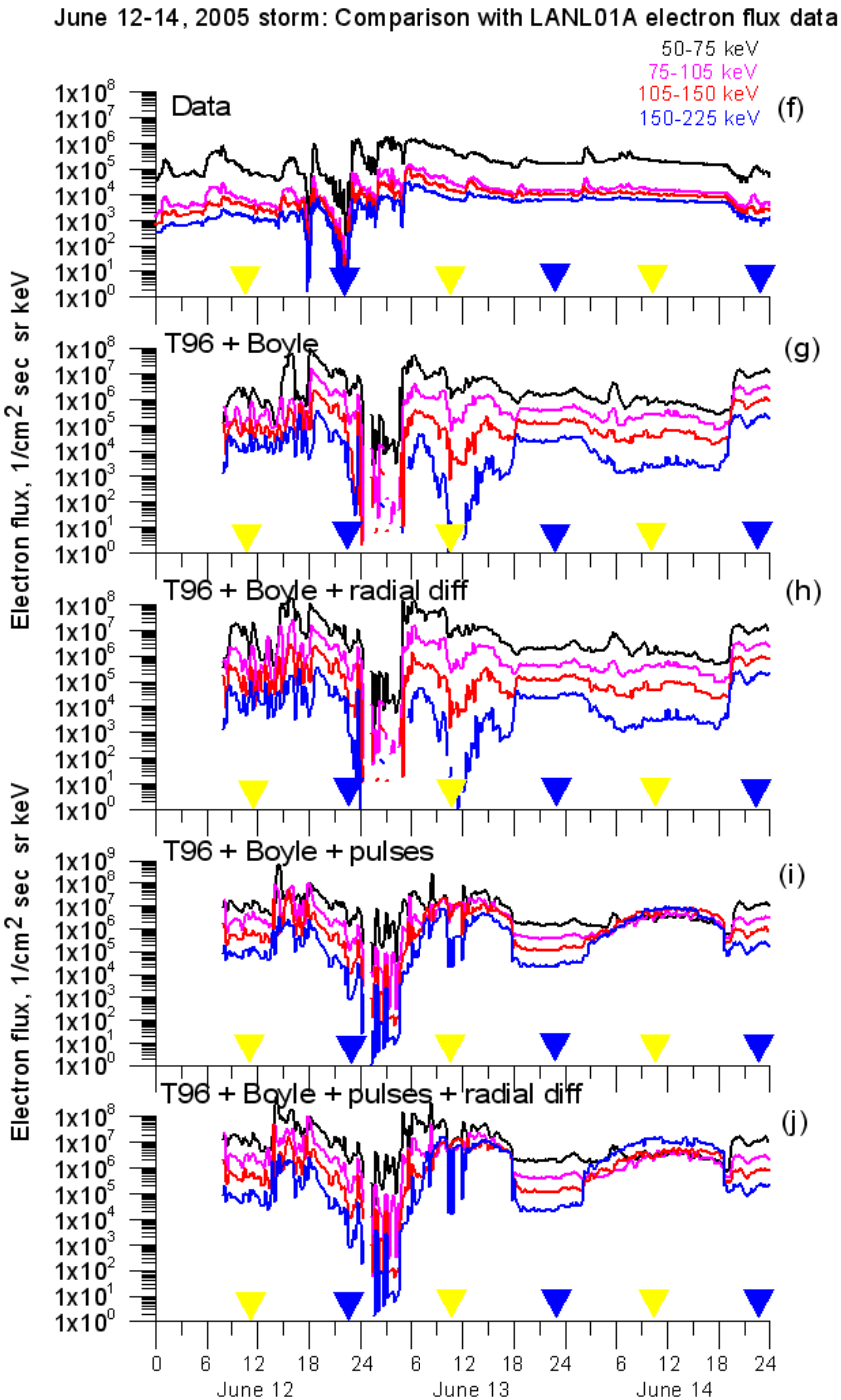

Relative roles of convection and substorm-associated electromagnetic fields at delivering plasma sheet electrons to the inner regions

Modeling with the **Inner Magnetosphere Particle Transport and Acceleration model (IMPTAM)**

Radial diffusion had no significant influence on the modelled electron fluxes.

We launch several pulses at the substorm onsets

Two orders of difference between the modelled electron fluxes and observed ones:
- low energy electron boundary conditions and
- loss processes due to WPI

Ganushkina at al., JGR, 2013

5-50 keV electrons during quiet event

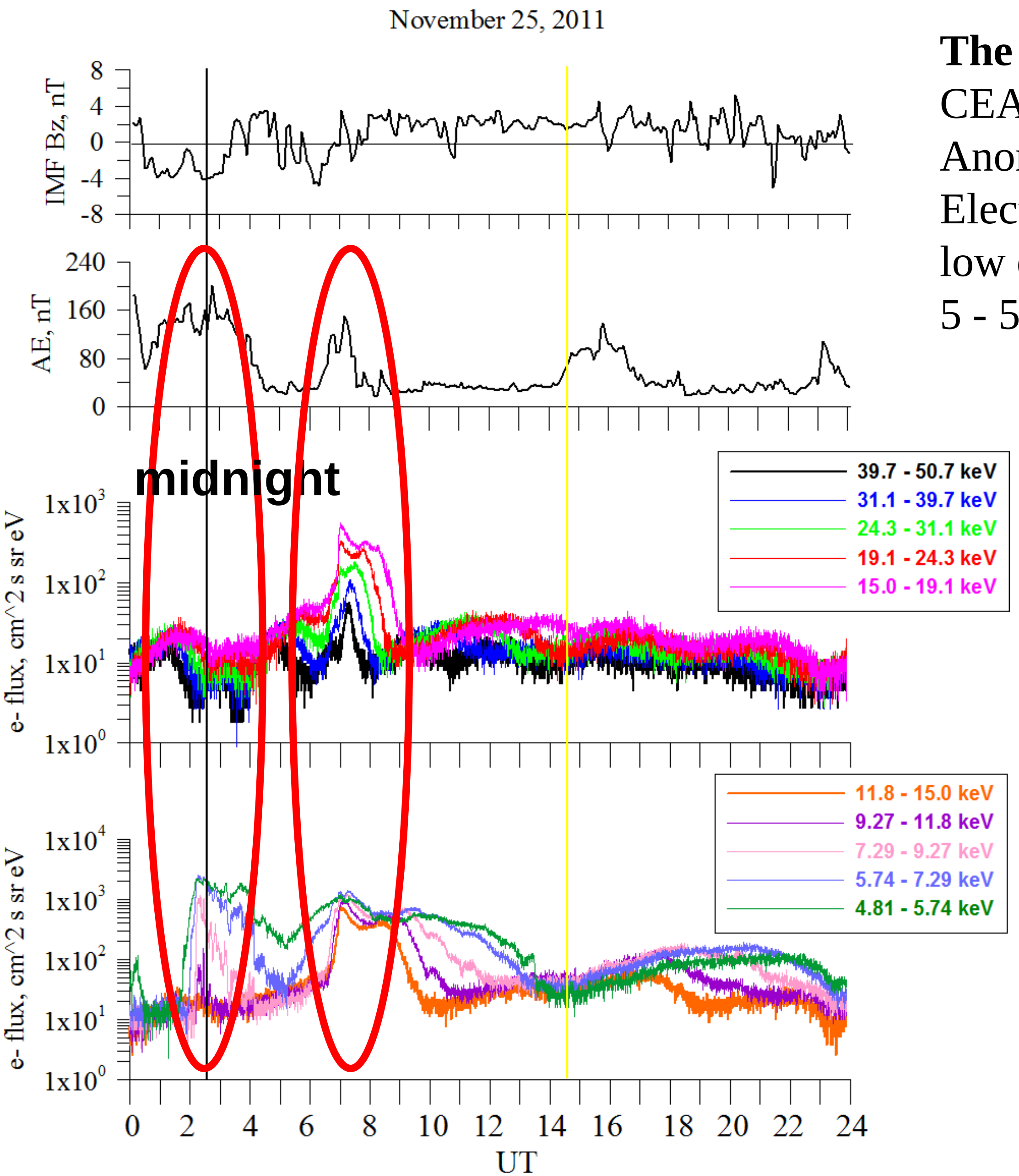

The data: AMC 12 geostationary satellite, CEASE-II (Compact Environmental Anomaly Sensor) instrument with Electrostatic Analyzer (ESA) for measuring low energy electron fluxes in 10 channels, 5 - 50 keV.

- **Flux increases** are related to **AE peaks** only (less than 200 nT, small, isolated substorms)

- The lower the energy, the large the flux and electrons of different channels behaves differently

- 1st peak (AE=200 nT) at midnight seen for energies > 11 keV

-2nd peak (AE=120 nT) at dawn, increase in all energies

Not a unique case

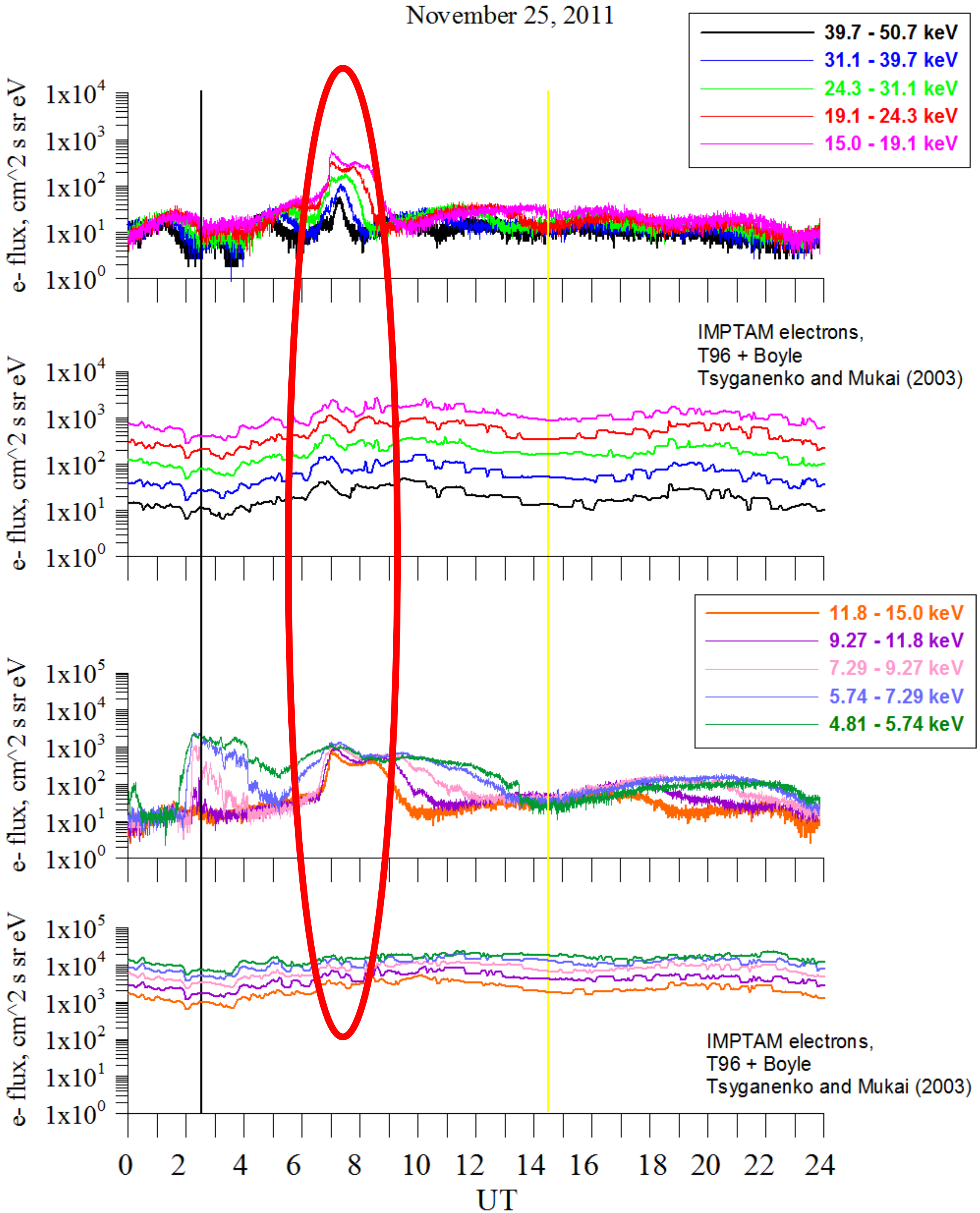

No significant variations in models' parameters –

no changes in modeled electron fluxes

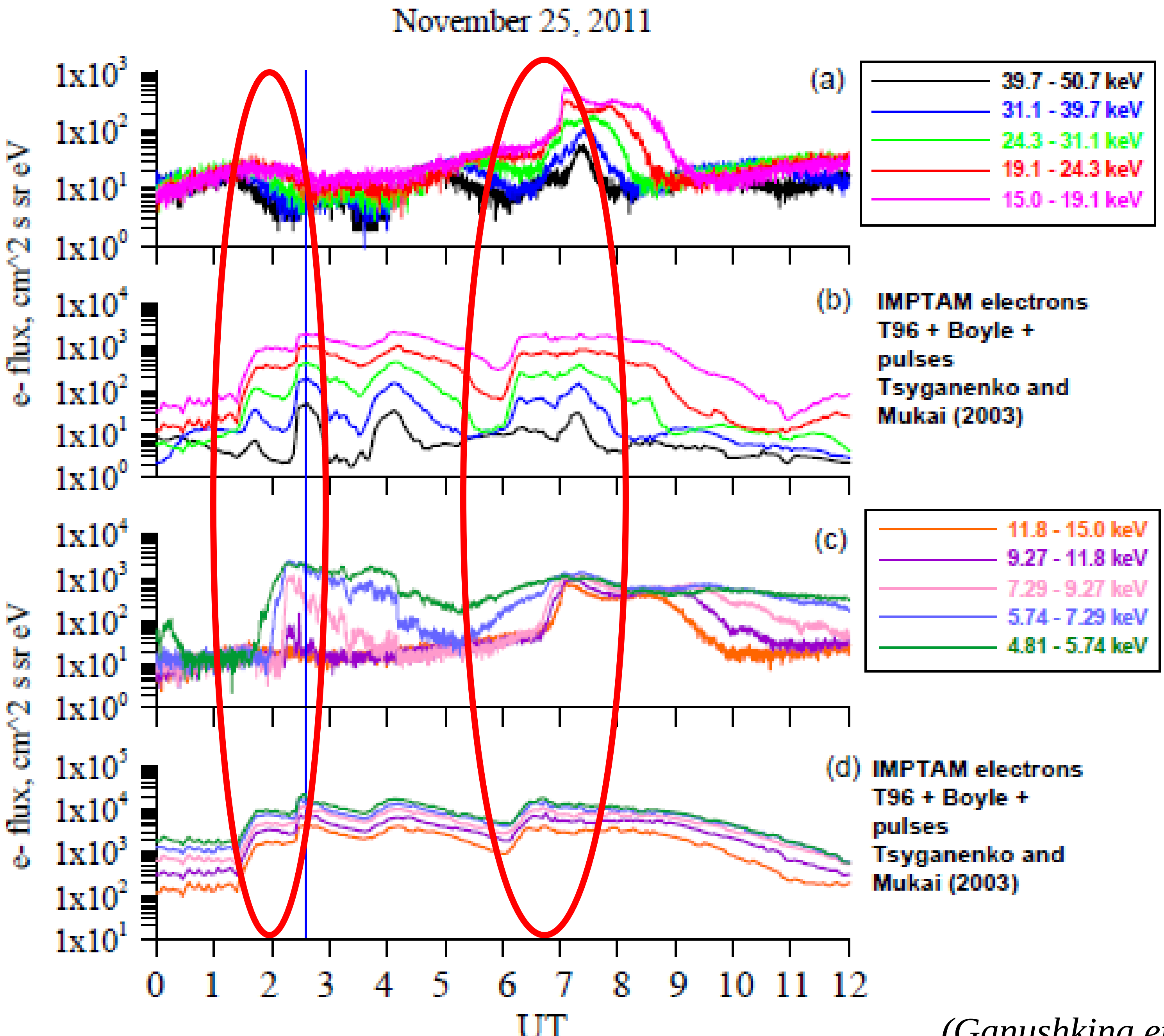

(Ganushkina et al., JGR, 2014)

Summarizing…

- Substorm-associated electromagnetic fields play a significant role in the particles' transport from the plasma sheet to the inner magnetosphere regions and acceleration

    Dispersed ion structures observed in the wide range of energies (eVs to tens of keVs) at many satellites

    - Provide important information on the electromagnetic fields and acceleration processes and particle transport
    - Substorm-associated electromagnetic pulses shift inward and accelerate existing population

    Concurrent action of large-scale convection and substorm-associated electromagnetic fields for ring current development

    Variations of fluxes for low energy electrons (5-50 keV) during non-storm period are due to substorm activity.

    - The increases in the observed fluxes can be captured when substorm-associated electromagnetic fields are considered
    - Modifications of the pulse model are needed, especially related to the pulse front velocity and arrival time.

Dipolarization fronts and pulsed electromagnetic fields

Recently, there have been quite a few studies on the dipolarization fronts observed during substorms (*Sergeev et al*., 2009; *Runov et al*., 2011; *Runov et al*., 2012; *Birn et al*., 2012). The main observational characteristics of these fronts include:

(1) rapid (about 1 to a few seconds) increase in Bz accompanied by rapid decrease in the plasma density, often preceded by a short Bz dip and followed by gradual Bz decrease at time scale of a minute;

(2) enhancement in electric field (up to about 10 mV/m) during a few tens of sec;

(3) gradual increase in energetic ion flux, which stars about 30 s ahead of the front;

(4) rapid, step-like increase or decrease in energetic electron flux.

There is no definite answer about the relationship (if any) between the fronts and the global substorm dipolarization observed at geosynchronous orbit. There exist some assumptions that the substorm dipolarization is a cumulative effect of braking fronts (*Lyons et al*., 2012). However, there is not enough evidence for that.

Dipolarization fronts do not penetrate deeper than geostationary distances (*A. Runov*, *private communication*, 2012). The origin of strong transient electric fields at substorm onset and their detailed relationship to the magnetic field dipolarization is still an open question.